Available online at www.sciencedirect.com

SciVerse ScienceDirect

Ceramics International 39 (2013) 991–997

CERAMICS INTERNATIONAL

www.elsevier.com/locate/ceramint

Sol–emulsion–gel synthesis of cordierite ceramics for high-frequency multilayer chip inductors☆

Shaohong Wang*, Haoran Lu, Zhaoxia Hou

Liaoning Province Key Laboratory of New Functional Materials and Chemical Technology, Shenyang University, Shenyang 110044, China

Received 22 August 2011; received in revised form 22 June 2012; accepted 4 July 2012
Available online 14 July 2012

Abstract

Nano-Cordierite powders used for high frequency chip inductors (MLCIs) were prepared by sol–emulsion–gel method. Effects of precursor concentration and [H_2O]/[Si] molar ratio on this material were studied. The sol–emulsion–gel processing of $Mg_2Al_4Si_5O_{18}$ as well as its dielectric property were investigated. Owing to the better packing efficiency and therefore higher surface energy of the freestanding nano-powder, the pressed pellets made by cordierite powder showed 98.6% theoretical density at 900 °C for 2 h. The additive Bi_2O_3 was utilized to promote the crystallization or transformation to α-cordierite and sintering. The sol–emulsion–gel-derived cordierite ceramics have low dielectric constant ($\varepsilon = 3.0 \sim 4.0$; 18 GHz) and low dielectric loss ($tg\delta < 0.001$; 18 GHz) and can be co-fired with high conductivity metals such as Au, Ag/Pd internal electrode at low temperature (900 °C), suggesting that it was an ideal dielectric material for high-frequency multilayer chip inductors.

Keywords: A. Sol–gel processes; C. Dielectric properties; D. Cordierite

1. Introduction

Multilayer chip inductors (MLCIs) are one of the key surface mounted devices in the circuit of the latest electronic products, such as notebook computers, camcorders, pagers and cellular phone, etc. [1–3]. Low-temperature sintered Ni–Zn–Cu ferrite has been used to fabricate the MLCIs for applications below 300 MHz. However, for applications in the radio frequency (RF) range, above 500 MHz to several GHz, the Ni–Zn–Cu [4] ferrite based chip inductors cannot be used due to the limitation of the self-resonant frequency of this material. For applications in the front end circuits in wireless telecommunication terminals the material and fabricated MLCIs with a higher self-resonant frequency are required. This material should have a low dielectric constant, low dissipation factor and low sintering temperature. At present, cordierite ($2MgO \cdot 2Al_2O_3 \cdot 5SiO_2$)-based ceramics are the most promising material used in high-frequency multilayer chip inductors due to their low dielectric constant, low dielectric loss, low thermal expansion coefficient, high mechanical strength and good electrical insulation properties [5–7]. The sintering temperatures of cordierite ceramics, prepared by the conventional glass melting, solid-phase sintering, sol–gel, precipitation parcel method and combustion synthesis method [8–15], are generally higher than 1000 °C, which can be co-sintered with copper internal electrode. In MLCIs applications, however, the materials must be sintered at temperature lower than 950 °C so as to co-fire with the high conductivity metal Ag internal electrode.

In order to achieve the aim, low temperature sintering of cordierite ceramics, the sol–emulsion–gel route, which is widely practiced for preparation of ceramic microspheres was investigated [16–17]. This method is notably recognized as a novel technique, which offers control over homogeneity as well as physical characteristics such as particle size, size distribution, degree of aggregation, and morphology.

☆This work was financially supported by the National Natural Science Foundation of China (No. 50702035), National Key Basic Research Development Plan of China (‘973’ Projects 2011CB612209) and Special Fund of Shenyang key laboratory construction (F10-216-1-00).

*Corresponding author.
E-mail address: lhr2006518@126.com (S. Wang).

0272-8842/$36.00 © 2012 Elsevier Ltd and Techna Group S.r.l. All rights reserved.
http://dx.doi.org/10.1016/j.ceramint.2012.07.017

In the present work, a modified sol–emulsion–gel process was developed for the synthesis of cordierite microspheres. The sol–emulsion–gel process involves sol generated from TEOS, aluminum nitrate nonahydrate and magnesium nitrate hexahydrate as aqueous phase, cyclohexane as the oil phase, Polyethylene glycol octyl phenyl ether (TritionX-100) as the surfactant and n-hexanol as the cosurfactant to enhance the emulsion formation. The pseudo ternary phase diagram of sol/Triton X-100/hexanol/cyclohexane, the effect of pH value, H_2O/TEOS (molar ratio) on the gelation time is presented. The sol–gel mechanism of cordierite and crystallization process is investigated as well.

2. Experimental procedure

The precursor materials for the preparation of magnesia–alumina sol with the $MgO:Al_2O_3$ molar ratios of 2:4 were magnesium nitrate hexahydrate, $Mg(NO_3)_2 \cdot 6H_2O$ (11.72 g, A.R., SCRC, China, purity $>$ 99%), and aluminum nitrate nonahydrate, $Al(NO_3)_3 \cdot 9H_2O$ (43.25 g, A.R., SCRC, China, purity $>$ 99%). An aqueous magnesia–alumina sol was prepared by dissolving the nitrate and Bi_2O_3 (5 wt%, A.R., SCRC, China, purity $>$ 99%) in deionized water (conductivity of deionized water: $1.2 \times 10^{-5}\ \Omega$/cm), adjusting the pH value to about 3 by the addition of concentrated ammonia solution (26 wt%, SCRC, China) and finally, heating the 2 M solution thus obtained to 45 °C under controlled condition, i.e. by dropwise addition of concentrated ammonia solution under vigorous stirring in a covered container. The proportional TEOS (30.03 g) was then added and stirred for 2 h in order to hydrolyze the hydrophobic C_2H_5O-groups to hydrophilic HO-groups, thus forming a homogeneous solution. The molar ratio of magnesia to alumina to silica in the tri-component and transparent sol was maintained at 2:2:5. The prepared sols were used as the aqueous phase (W) while an organic solvent, i.e. the cyclohexane was used as the oil phase (O), polyethylene glycol octyl phenyl ether as the surfactant and n-hexanol as the cosurfactant to enhance the emulsion formation. The emulsions were prepared by dispersing the sol as droplets in the support solvent under constant agitation (180 rpm). The mass ratio of TritonX-100/n-hexanol/cyclohexane was 2:1:2. The volume ratio of the sol:support solvent was kept constant at 1:4 in all experiments. The emulsified sol droplets were converted to gel microspheres by the addition of an extractant (gelling agent) e.g. triethylamine. The volume ratio of the sol to the gelling agent was about 2:1. The gel particles were separated by centrifugation followed by washing with acetone and methanol. The product thus obtained was dried at 120 °C in an air oven for 10 h and finally calcined at 650 °C with 2 h dwell time. The flow chart for microsphere synthesis was provided in Fig. 1.

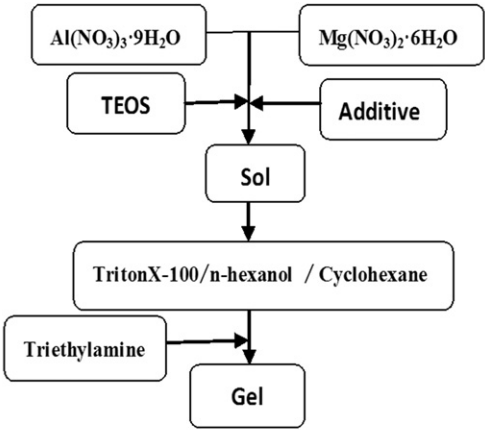

Fig. 1. Flow chart of cordierite microsphere derived from sol–emulsion–gel.

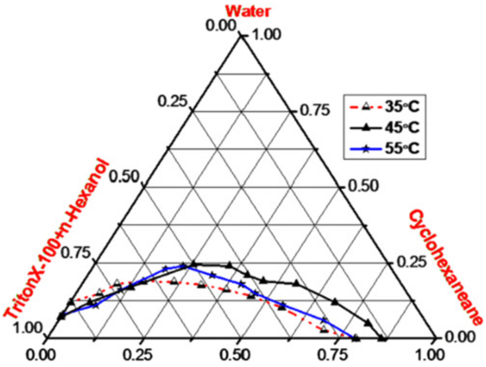

Fig. 2. Pseudo ternary phase diagram for the reverse micro-emulsion at different temperature.

The powder particle size distribution was characterized by laser particle size analyzer (Mastersizer 2000), DSC and TG of powders were analyzed by the United States Dupon high temperature thermal analysis apparatus (from 30 to 1000 °C with a heating rate of 10 °C/min in argon atmosphere under a flow rate of 0.70 ml/min in alumina crucible). Crystalline phases were identified by Rigaku D Max-type X-Ray diffractometer (Cu $K\alpha$, 40 kV, 30 mA, step size 0.02°). Micro-structure of sintered samples (semi-pressure to Ø15 mm wafer) was observed by SEM-JSM-6301F. High-resolution TEM(JEM-3200FSC) images were obtained in a high-voltage electron microscope operated at 1250 kV. For the dielectric measurements, Ag electrodes were screen printed with Ag pastes on both sides of the pellets and heat treated at 550 °C for 2 h. The frequency dependence of the dielectric constant and dielectric loss was measured by an HP 4192A impedance analyzer (Palo Alto, CA) over a frequency range from 100 MHz to 20 GHz.

3. Results and discussion

The pseudo ternary phase diagram for sol/Triton X-100/hexanol/cyclohexane at 35 °C, 45 °C and 55 °C was surveyed and drew precisely, shown in Fig. 2. It showed that the effect of temperature on the W/O phase region was unconspicuous, and when the temperature was at 45 °C, the W/O phase region was relatively broad and the amount of aqueous phase was increased considerably. As for the effect of reaction temperature on the non-ionic surfactant TritonX-100, when temperature increased, the strength of hydrogen bond between oxygen atoms of oxyethylene groups and water molecules was weakened heavily, the hydrophilcity of TritonX-100 surfactant was weakened correspondingly, and ability to form W/O micro-emulsion of this system was weakened.

Therefore the preparation of various nano-powders usually was reacted under the condition of alkali catalysis. $NH_3 \cdot H_2O$ was used as the catalyst here, and the effect of pH value, H_2O/TEOS (molar ratio) on the gel time was studied.

It can be seen from Fig. 3 that the fastest gelation time (only 4.2 h) was corresponding to pH 5.0. Alkoxide hydrolysis process required water, while the condensation process produced water, so more or less water added through both affected the gelation time. As showed in Fig. 4, it was found that the gelation time was the shortest when H_2O/TEOS (molar ratio) was around 4.3. In the circumstance of alkali catalysis, the interaction of the hydroxyl, silicon alcohol and water molecules generated $Si(OH)_6^{2-}$ complex ion. Then the neutralization reaction was executed among complex ion, Al^{3+} and Mg^{2+}, and then through the reaction of polymerization to generate $2[Mg^{2+}][Si(OH)_6]_2^{2-}4[Al^{3+}][Si(OH)_6]_3^{2-}(OH^-)_6$. The overall reaction was as followed.

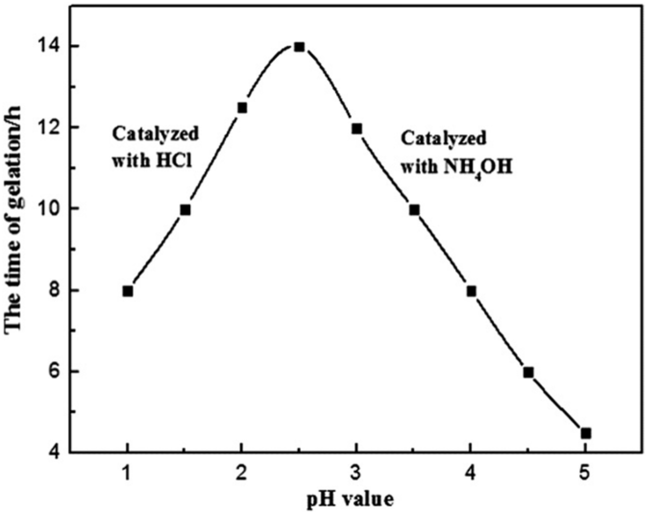

Fig. 3. Effect of pH value on gelation time.

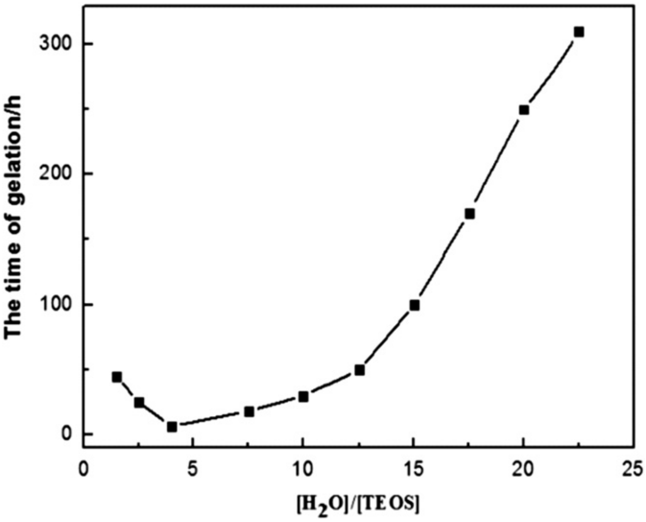

Fig. 4. Effect of $[H_2O]/[Si]$ molar ratio on gelation time.

$$5Si(OC_2H_5)_4 + 2Mg^{2+} + 4Al^{3+} + 17H_2O + 16OH^-$$
$$\rightarrow 5[Si(OH)_6]^{2-} + 2Mg^{2+} + 4Al^{3+} + 20C_2H_5OH$$
$$\rightarrow 2[Mg^{2+}][Si(OH)_6]_2^{2-}4[Al^{3+}][Si(OH)_6]_3^{2-}(OH^-)_6$$
$$+ 20C_2H_5OH \rightarrow Mg_2Al_4Si_5O_{18} + 20C_2H_5OH + 15H_2O$$

The particle size and distribution of powder annealed at 650 °C for 2 h was shown in Fig. 5. It can be seen that the distribution of particle size was concentrated, and the effective diameter prepared by sol–emulsion–gel method was about 25 nm. Compared with sol–gel method, the degree of agglomeration was lower. In the sol–gel processing, if the $[H_2O]/[Si]$ molar ratio was smaller or the pH value of mixed solution was larger, it often led to rapid hydrolysis and condensation, and it would generate a large number of primary particles (20 nm or so) with high reunion, shown in Fig. 6a_2. While the hydrolysis and condensation of the precursor in the process of sol–emulsion–gel method was limited in the water nuclear of W/O micro-emulsion, primary particles was prevented from congregating by the oil phase around, which made the formation of agglomeration more difficult, so the size of prepared particles was finer and the morphology was well proportioned, shown in Fig. 6a_1.

DSC–TG curve of powder dried at 80 °C was shown in Fig. 7. The sharp weight loss appears at temperature range of 100–550 °C and tends to stop at around 650 °C. The

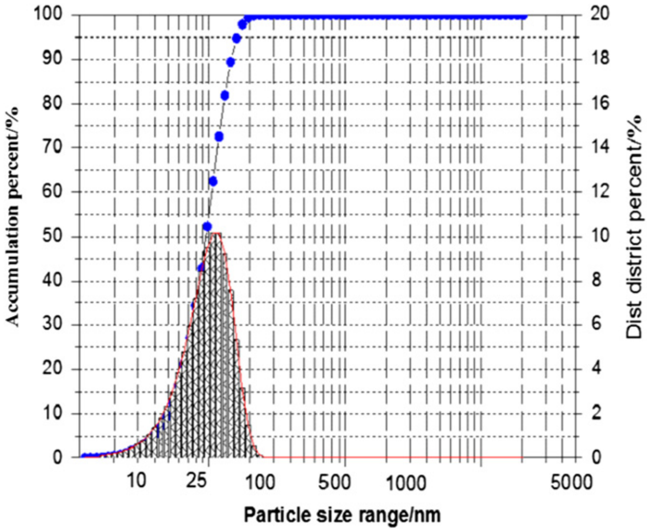

Fig. 5. Distribution of cordierite particle size prepared by sol–emulsion–gel method.

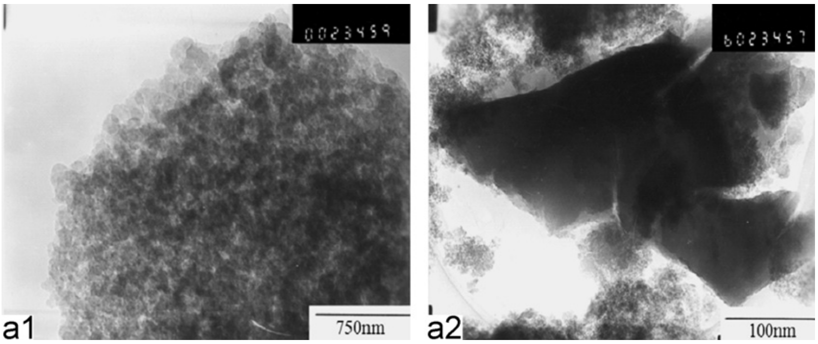

Fig. 6. TEM micrographs of powders (a_1) sol–emulsion–gel method; (a_2) sol–gel method.

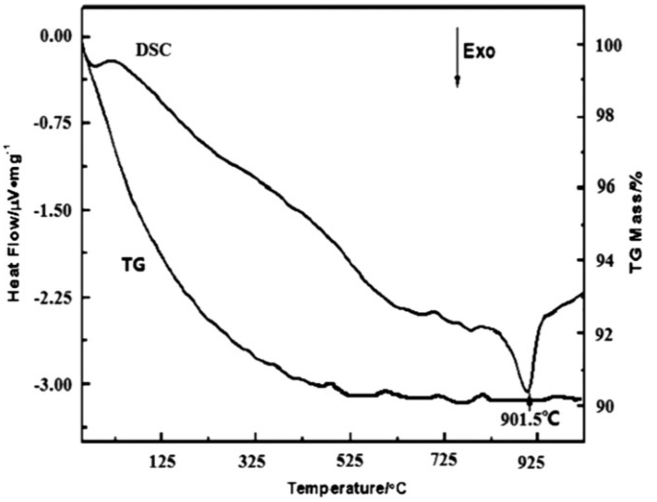

Fig. 7. DSC–TG patterns of powder calcined at 650 °C.

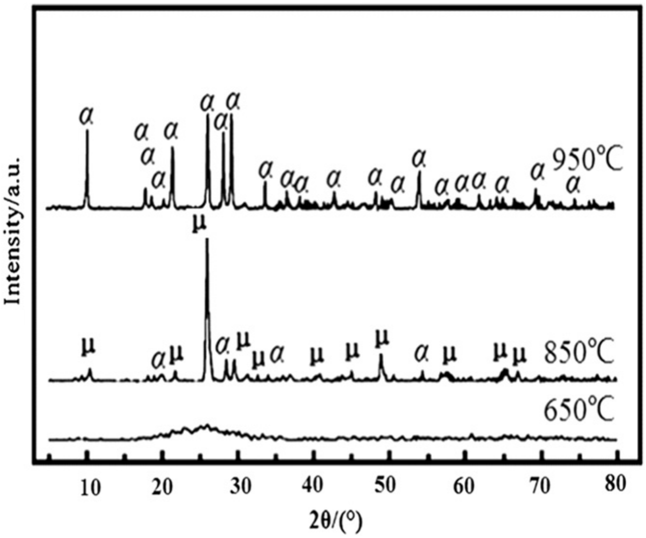

Fig. 8. XRD patterns for sintered samples at different temperatures.

substantial weight loss results from the release of H_2O gas and CO_2 due to the decomposition of TEOS precursor. XRD of samples sintered at different temperatures was shown in Fig. 8, the obvious crystallization peak around 901 °C was corresponding to the precipitation α-cordierite. It was found that powders crystallization process: amorphous → μ-cordierite → α-cordierite. It is still amorphous when heated at 650 °C, and crystallization occurs mainly with μ-cordierite and a small amount of α-cordierite at 850 °C. The metastable phase μ-cordierite transforms completely to α-cordierite at 950 °C. There was no spinel ($MgAlO_4$), mullite ($Mg_2Al_6O_{13}$) and other impurity phases in the whole region of crystallization, because the powder prepared by sol–emulsion–gel was with high activity, large surface energy, and low reunion, which promoted α-cordierite to devitrify directly from metastable phase μ-cordierite and decreased the precipitated opportunities of other crystalline phases. The Bi_2O_3 additive existed in the amorphous state could increase the activity of the powders further, meanwhile Bi_2O_3 could provide positions for heterogeneous nucleation, decrease the nucleation temperature of base body and promote powder crystallization. Bi^{3+} ionic radius($r=0.096$ nm) and its relative atomic mass was larger, whereas the *c*-axis of μ-cordierite was not long enough to accommodate Bi^{3+}, and it was difficult for dendritic μ-cordierite in the matrix to migrate Bi^{3+}, to some extent, Bi^{3+} largely restrained μ-cordierite nucleation and growth, so α-cordierite with long *c*-axis could crystallize directly and the temperature of phase transformation is consequently lower [18].

It can be seen from Fig. 9 that the fracture surface was dense and of low porosity. It can be concluded that the density of sample sintered at 900 °C reaches 98% theoretical density according to the measurements of sintered body density by Archimedes method. The microstructure of this ceramic material was mainly composed of the large number of micron-sized grains and very few pores (Fig. 9b), which was just an ideal microstructure for dielectric materials used in the field of high-frequency multi-layer chip inductors.

It was shown in Fig. 10 that the dielectric constant and dielectric loss properties had both been reduced with the increased sintering temperature, and the dielectric properties ($\varepsilon \sim 4.0$, $tg\delta < 0.001$; 18 GHz) of the samples sintered at 900 °C was the best. Materials with low dielectric constant can reduce relaxation time and cross-interference in the

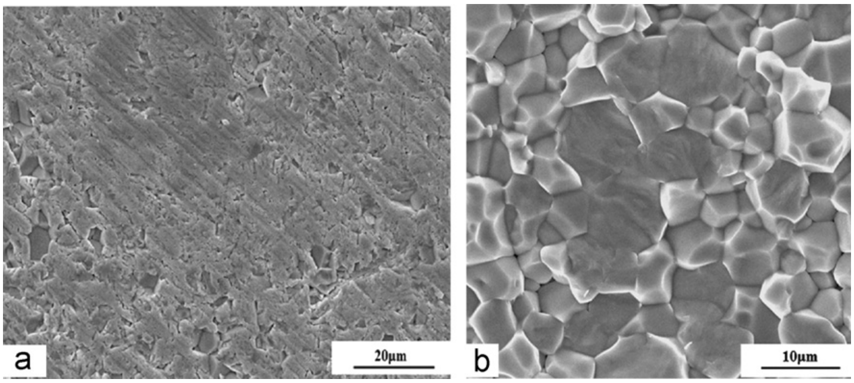

Fig. 9. SEM micrographs of cordierite sintered at 900 °C for 2 h (a) surface SEM and (b) fracture surface SEM.

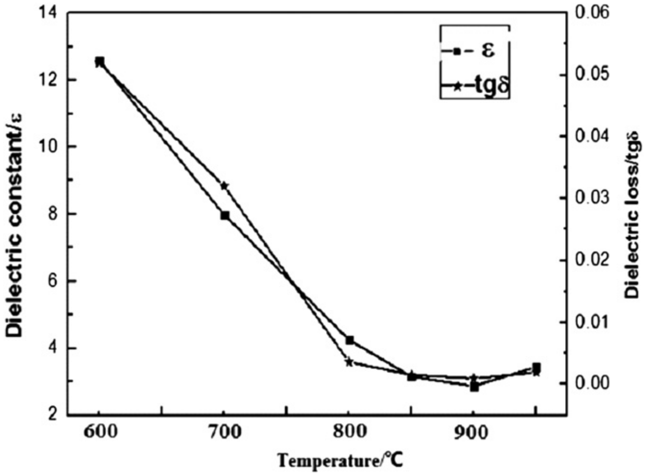

Fig. 10. The dielectric constant and dielectric loss of sintered samples at different temperature.

process of signal transmission, while low dielectric loss was essential for the high frequency chip inductor materials to reduce thermal losses and promote heat dissipation under the circumstance of high frequency and larger resistivity. As a result, the material could be sintered at lower temperature and have very low dielectric constant and dielectric loss, which could match to the requirement of high frequency chip inductor.

The calcined powders derived from sol–emulsion–gel method were compressed under a pressure of 100 Mpa into $Ø10 \times 4\,\mathrm{mm}^2$ green cylinder. Cordierite green casting bodies were printed with silver paste by screen printing process, and were co-sintered at 900 °C for 2 h in air stove. After cooling the morphology of co-firing interfaces were observed, and the external silver electrode of co-sintered ceramic body was sprawled smoothly without flaw which demonstrated that shrinking percentage of dielectric material and silver electrode was consistent. Co-firing interfaces between cordierite dielectric ceramics and silver electrode and the distribution of elements at the interfaces were shown in Fig. 11, it can be seen that the co-sintered interfaces between cordierite and silver electrode were highly dense without crackle and pore. The elements distribution of Mg, Al, Si and O at the interfaces of cordierite and silver electrode were well-distributed.

The frequency dependence of the dielectrical property for sintered sample was showed in Fig. 12. The cut-off frequency came to 18 GHz. Cut-off frequency is defined as the corresponding frequency when dielectric loss of ceramic materials came up to maximum value. The samples sintered at 900 °C for 2 h were equipped with low dielectric constant and dielectric loss ($\varepsilon = 4.38$, $tg\delta = 0.00011$; 18 GHz) which was qualified for low temperature co-firing (< 950 °C) with silver electrodes, and it was the ideal dielectric materials used for high frequency chip inductor components.

4. Conclusions

The raw materials TEOS, aluminum nitrate, magnesium nitrate, ethanol and ultrapure water were used to prepare a precursor sol that was then dissolved in the emulsion of TritonX-100/n-hexanol/cyclohexane to synthetize high quality cordierite gel. The optimal combination of the treating temperature, and the ratio of $[H_2O]/[Si]$ were found to be 45 °C and 4.3, respectively. $NH_3 \cdot H_2O$ was an effective catalyst in the hydrolytie and polycondensation processing of tetraethyl orthosilicate. We have investigated the crystallization behavior of cordierite-derived from sol–emulsion–gel method and can conclude that the stable α-cordierite can be directly crystallized from amorphous state. It is found that Bi_2O_3 is a necessary sintering aid for low-temperature cosintering, and Bi^{3+} restrains μ-cordierite from nucleating and growing.

The sol–emulsion–gel-derived cordierite ceramics have low dielectric constant ($\varepsilon \sim 4.0$; 18 GHz) and low dielectric loss ($tg\delta < 0.001$; 18 GHz) and can be co-fired with high conductivity Ag internal electrode at 900 °C for 2 h. The cordierite co-sintered with silver electrodes at 900 °C for 2 h is the ideal dielectric material for making high frequency chip inductor components (MLCIs).

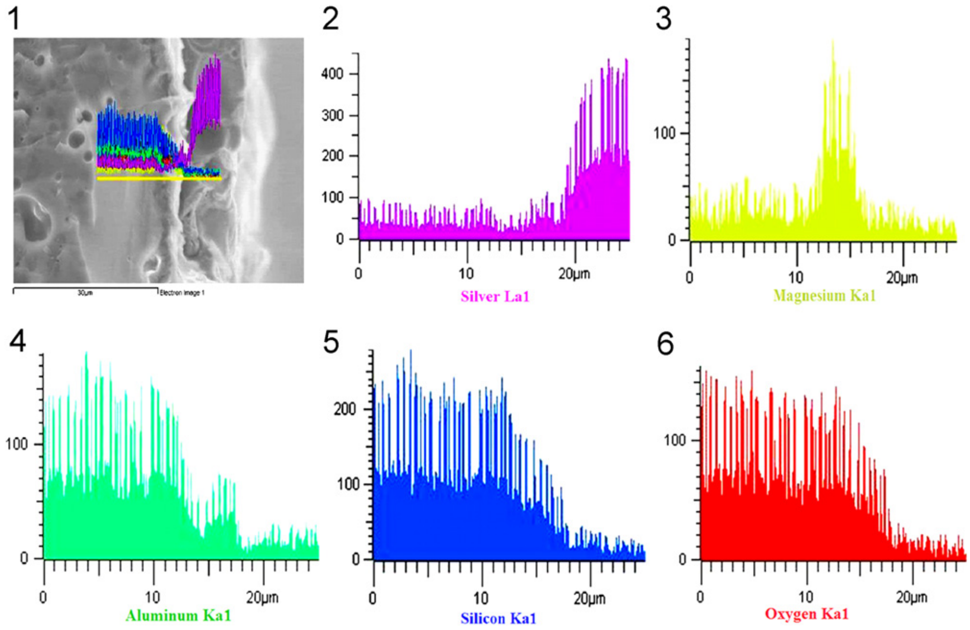

Fig. 11. (1) Co-firing interfaces between cordierite dielectric ceramics and silver electrode at 900 °C for 2 h. (2) The distribution of silver element at the interfaces between cordierite dielectric ceramics and silver electrode. (3) The distribution of magnesium element at the interfaces between cordierite dielectric ceramics and silver electrode. (4) The distribution of aluminum element at the interfaces between cordierite dielectric ceramics and silver electrode. (5) The distribution of silicon element at the interfaces between cordierite dielectric ceramics and silver electrode. (6) The distribution of oxygen element at the interfaces between cordierite dielectric ceramics and silver electrode.

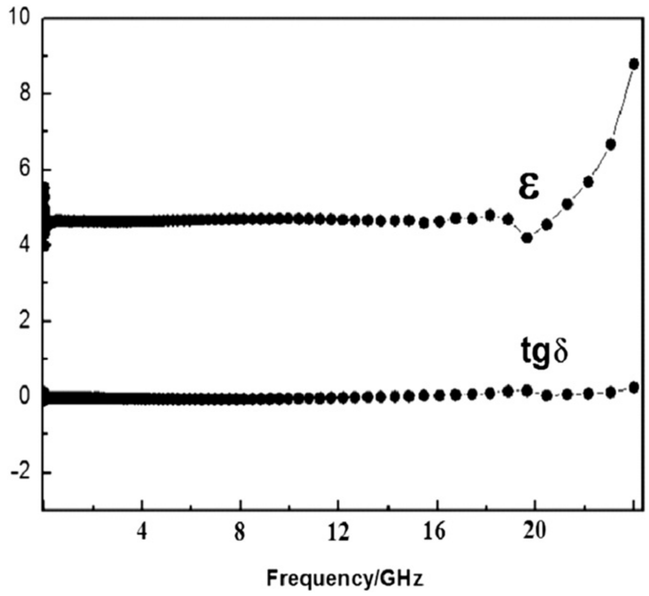

12. The frequency dependence of the dielectrical property for sintered sample (900 °C, 2 h).

References

[1] M.A. Gabal, Abdullah M. Asir, Y.M. AlAngari, On the structural and magnetic properties of La-substituted Ni–Cu–Zn ferrites prepared using egg-white, Ceramics International 37 (2011) 2625–2630.

[2] X.H. Wang, W.G. Qu, L.T. Li, et al., The influence of Mn dopant on the electromagnetic properties of Ni–Cu–Zn ferrite, Ceramics International 30 (2004) 1615–1618.

[3] M.C. Dimri, S.C. Kashyap, D.C. Dube, High frequency behaviour of low temperature sintered polycrystalline Ni–Cu–Zn ferrites and their composite thick films, Journal of the American Ceramic Society 207 (2010) 396–400.

[4] M.M. Eltabey, K.M. El-Shokrofy, S.A. Gharbia, Enhancement of the magnetic properties of Ni–Cu–Zn ferrites by the non-magnetic Al^{3+}-ions substitution, Journal of Alloys and Compounds 509 (2011) 2473–2477.

[5] Y.S. Cho, W.A. Schulze, V.R.W. Amarakoon, Crystallization kinetics and properties of nonstoichiometric cordierite-based thick-film dielectrics, Journal of the American Ceramic Society 82 (1999) 3186–3192.

[6] M.R. Barati, Influence of zinc substitution on magnetic and electrical properties of MgCuZn ferrite nanocrystalline powders prepared by sol–gel, auto-combustion method, Journal of Alloys and Compounds 478 (2009) 375–380.

[7] L.H. Luo, H.P. Zhou, C. Xu, Microstructural development on sol–gel derived cordierite ceramics doped B_2O_3 and P_2O_5, Materials Science and Engineering: B 99 (2003) 348–351.

[8] M.K. Naskar, M. Chatterjee, Magnesium aluminate ($MgAl_2O_4$) spinel powders from water-based sols, Journal of the American Ceramic Society 88 (2005) 38–44.

[9] J.M. Wu, S.P. Hwang, Effects of (B_2O_3, P_2O_5) additives on microstructural development and phase-transformation kinetics of stoichiometric cordierite glasses, Journal of the American Ceramic Society 83 (2000) 1259–1265.

[10] M.G.M.U. Ismail, H. Tsunatori, Z. Nakai, Preparation of mullite cordierite composite powders by the sol–gel method: its characteristics and sintering, Journal of the American Ceramic Society 73 (1990) 537–543.

[11] S.P. Hwang, J.M. Wu, Effect of composition on microstructural development in MgO–Al_2O_3–SiO_2 glass-ceramics, Journal of the American Ceramic Society 84 (2001) 1108–1112.

[12] A. Salinas, S.J. Castillo, F.F. Castillón-Barraza, Víctor M. Castaño, Synthesis and characterization of hydroxyapatite–wollastonite

composite powders by sol–gel processing, International Journal of Applied Ceramic Technology 5 (2008) 401–411.

[13] K. Morinaga, H. Takebe, Crystallization processes of cordierite glasses, Journal of the American Ceramic Society 100 (1996) 1423–1427.

[14] R.R. Tummala, Effect of composition on microstructural development in $MgO–Al_2O_3–SiO_2$ glass-ceramics, Journal of the American Ceramic Society 74 (1991) 895–980.

[15] R. Ianos, I. Lazau, C. Pacurariu, Solution combustion synthesis of α-cordierite, Journal of Alloys and Compounds 480 (2009) 702–705.

[16] H.J. Lee, J.H. Song, J.H. Kim, Synthesis of resorcinol/formaldehyde gel particles by the sol–emulsion–gel technique, Material Letters 37 (1998) 197–200.

[17] X.M. Yang, T.K. Chaki, Hollow lead zirconate titanate microspheres prepared by sol–gel/emulsion technique, Materials Science and Engineering: B 39 (1996) 123–128.

[18] S.H. Lo, C.F. Yang, The sintering characteristics of Bi_2O_3 added $MgO–CaO–Al_2O_3–SiO_2$ glass powder, Ceramics International 24 (1997) 139–144.